Maximizing the Capacity of Magnetic Induction Communication for Embedded Sensor Networks in Strongly and Loosely Coupled Regions

Kisong Lee and Dong-Ho Cho

Chips(N26) 110, Department of Electrical Engineering, Korea Advanced Institute of Science and Technology (KAIST), Daejeon 305-701, Korea

We attempt to maximize the capacity of magnetic induction communication in strongly and loosely coupled regions. In a strongly coupled region, we investigate frequency splitting, which disturbs the resonance of transmitter and receiver coils. We find a splitting coupling point, which is the value just before frequency splitting occurs, and propose an adaptive frequency-tracking scheme for finding an optimal frequency. The proposed scheme compensates for the degradation of capacity and so guarantees large capacity even at regions where frequency splitting occurs. Next, in a loosely coupled region, we derive an optimal quality factor for maximizing capacity in a two-coil system. As the distance between coils increases, strong resonance is needed to overcome the serious attenuation of signal strength. As a result, the optimal quality factor should be increased. In addition, we find an optimal quality factor for a relay system in order to guarantee reliable communication at long distance. In addition, an optimal-Q scheme that adjusts the optimal quality factor according to a given distance can achieve near-optimal capacity. Finally, through simulations using the Agilent Advanced Design System, we demonstrate the accuracy of our analytic results and the effectiveness of the proposed schemes.

Index Terms—**Embedded sensor networks, frequency splitting, magnetic induction communication, quality factor.**

I. Introduction

RECENTLY, for various purposes, sensor networks have been deployed in which the sensors are embedded in dense media including rock, soil, and water. For example, in ubiquitous home networks, sensors are embedded in the walls of building for convenience and aesthetic reasons [1]. In addition, sensors are sometimes buried underground so that environmental conditions, the state of infrastructure, and other situations can be monitored [2]. Traditional wireless communication uses electromagnetic (EM) waves to convey information. However, EM waves are not appropriate for communication in dense media for three major reasons: high path loss, dynamic variation in the channel, and large antenna size [3], [4]. In contrast, communication using magnetic induction (MI), in which information is transferred between coil antennas, does not suffer from these problems and so is promising for use in embedded sensor networks. In air, the power of magnetic fields falls in proportion to $1/d^6$, while the power of EM waves falls in proportion to $1/d^2$ as the distance d increases in the near-field region [4]. However, the magnetic permeability of dense media is similar to that of air, so the propagation loss of magnetic fields caused by absorption is smaller than that of the EM waves in dense media [2], [5]. This characteristic of magnetic fields compensates for the attenuation of signal strength in dense media.

MI communication has been studied intensively. In [2] and [3], the characteristics of the underground channel and challenges for the use of MI communication in wireless underground sensor networks (WUSNs) were identified. In [6] and [7], an MI waveguide, which consists of linear arrays of double-sided elements, was investigated and found to have low propagation loss and reflection. In [4], the authors analyzed the path loss of MI communication. In addition, they considered an MI waveguide in which relay coils are deployed at equal intervals between transmitter and receiver coils to increase communication range and investigated the path loss of the MI waveguide. In [8], algorithms for deploying sensors were proposed to enable an MI waveguide for WUSNs to be connected to the network. In [9] and [10], the capacity of a near-field communication system was analyzed using an equivalent circuit model as a basis. The authors provided good guidelines for estimating capacity performance and antenna design. However, they were not able to provide simulation results for verifying the accuracy of numerical results as well as a closed-form solution for maximizing capacity. Most previous works focused on the increase of communication range, but there was no solution to increase the low capacity of MI communication. In WUSNs, a low data rate of several kilobits per second (kb/s) is sufficient to support simple monitoring applications [2]. However, some applications, such as home networks, require a high data rate [11]. Thus, network capacity is the most important issue that needs to be addressed regarding MI communication.

In this paper, we focus on maximizing the capacity of networks that use MI communication. Here, we present a model of a magnetically coupled communication system using an equivalent circuit model. In addition, our contributions can be described as follows.

i) In a strongly coupled region, we investigate frequency splitting in view of the MI communication, in which a resonant frequency is separated into two frequency modes, one higher and the other lower than the original resonant frequency. Here, we find the splitting coupling point, which is the value of coupling coefficient just before frequency splitting occurs. In addition, we propose an adaptive frequency-tracking scheme, which finds the optimal

Manuscript received January 07, 2013; revised March 29, 2013; accepted April 05, 2013. Date of publication April 18, 2013; date of current version August 21, 2013. Corresponding author: K. Lee (e-mail: kslee@comis.kaist.ac.kr).

Digital Object Identifier 10.1109/TMAG.2013.2258933

frequency to guarantee large capacity, even in the presence of frequency splitting.

ii) In a loosely coupled region, we derive the channel model near the resonant frequency, which includes fading as well as path loss. Using this channel model as a basis, we find the closed-form expression of an optimal quality factor for maximizing capacity in a two-coil system. We also consider an MI relay system to support large capacity when transmitting over long distances. Expanding the analytical results for the two-coil system, we also derive the closed-form expression of an optimal quality factor for maximizing capacity in the MI relay system. We find that the optimal quality factor should be increased for maximizing capacity at long distances in order to compensate for the serious attenuation of signal strength.

iii) Using the Agilent Advanced Design System (ADS), we perform simulations to demonstrate the accuracy of our numerical analysis. The analytical results are in good agreement with the simulation results. In addition, we show that capacity can be improved significantly by changing an original center frequency to the optimal frequency when frequency splitting occurs. Further, an optimal-Q scheme that tunes the optimal quality factor at a given distance achieves larger capacity, which is near-optimal performance, than a conventional fix-Q scheme at all distances.

The remainder of the paper is organized as follows. In Section II, the model of the system that uses MI communication is described, and frequency splitting is investigated in a strongly coupled region. In Section III, the optimal quality factors for both the two-coil system and the relay system are derived using the channel model in the loosely coupled region. In Section IV, the performance of the proposed schemes is evaluated. Finally, conclusions are made in Section V.

II. Strongly Coupled Region

Fig. 1(a) shows a block diagram of the MI communication system. Here, the transmitter coil (Tx coil) and the receiver coil (Rx coil) are centered on a single axis. The radii of Tx coil and Rx coil are a_t and a_r, respectively, and d is the distance between the two coils. Fig. 1(b) shows the equivalent circuit model. V_t is an alternating voltage that has an angular frequency ω. Here, $\omega = 2\pi f_c$ and f_c is a resonant frequency. In addition, f_c is used as a central frequency for the MI communication; L_t and L_r are the self-inductances of the Tx coil and Rx coil, respectively; r_{lt} and r_{lr} are the resistances of the coils; C_t and C_r are the capacitances that make two coils resonate at the same frequency; and R_S and R_L are the source resistor and load resistor, respectively.

In MI communication systems, the communication link is formed by magnetic induction between two coils. For example, a sinusoidal current $i_t(\omega)$, which has an angular frequency ω, is generated from the voltage source V_t in the Tx coil. This current induces another sinusoidal current $i_r(\omega)$ in the Rx coil, thereby making MI communication possible. This inductive relationship

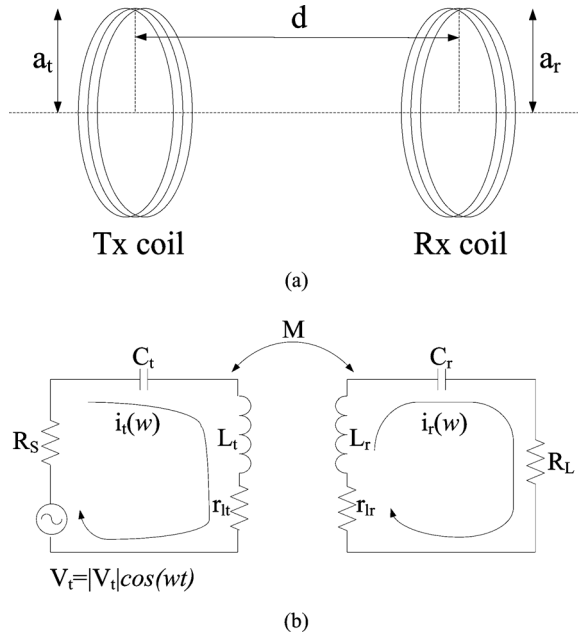

Fig. 1. System model of magnetically coupled MI communication. (a) MI communication system, (b) Equivalent circuit model.

between two coils can be represented by mutual inductance M, as follows:

$$M = \frac{\pi \mu_0 N_t N_r a_t^2 a_r^2 |\cos \theta_{tr}|}{2(a_t^2 + d^2)^{3/2}} \tag{1}$$

where μ_0 is the permeability of free space, N_t and N_r are the number of turns of Tx coil and Rx coil, respectively, and θ_{tr} is the angle between the axes of Tx and Rx coils, which pass through the centers of the coils. Also, the coupling coefficient can be estimated using the following equation:

$$k = \frac{M}{\sqrt{L_t L_r}}. \tag{2}$$

If the condition $(k^2 \omega_o^2 L_t L_r)/(r_{lt} r_{lr}) > 1$ is satisfied, the two coils are strongly coupled [12]. Otherwise, they are loosely coupled. In a strongly coupled region, the effect of coupling, which is seen in both the Tx and Rx coils, should be considered. Then, we can build the following node equations from Kirchhoff's voltage law (KVL):

$$\begin{aligned} V_t &= (R_S + r_{lt} + j\omega L_t + 1/j\omega C_t) i_t + j\omega M i_r, \\ 0 &= (R_L + r_{lr} + j\omega L_r + 1/j\omega C_r) i_r + j\omega M i_t. \end{aligned} \tag{3}$$

From (3), the currents generated in the Tx coil and the Rx coil can be obtained as follows:

$$\begin{aligned} i_t(\omega) &= \frac{V_t}{(R_S + r_{lt} + j\omega L_t + 1/j\omega C_t) + \left(\frac{\omega^2 k^2 L_t L_r}{R_L + r_{lr} + j\omega L_r + 1/j\omega C_r} \right)} \\ i_r(\omega) &= \frac{j\omega k \sqrt{L_t L_r}}{R_L + r_{lr} + j\omega L_r + 1/j\omega C_r} \cdot i_t(\omega). \end{aligned} \tag{4}$$

Here, we assume that both the Tx coil and the Rx coil have the same angular resonant frequency, which is defined as

$$\omega_o = \frac{1}{\sqrt{L_t C_t}} = \frac{1}{\sqrt{L_r C_r}}. \tag{5}$$

Then, we can obtain $i_t(\omega)$ and $i_r(\omega)$ near the angular resonant frequency using the first-order Taylor series expansion:

$$i_t(\omega) = \frac{V_t}{(R_S + r_{lt})(1 + j2\Delta\omega Q_t) + \left(\frac{\omega^2 k^2 L_t L_r}{(R_L + r_{lr})(1 + j2\Delta\omega Q_r)}\right)}$$
$$i_r(\omega) = \frac{j\omega k\sqrt{L_t L_r}}{(R_L + r_{lr})(1 + j2\Delta\omega Q_r)} \cdot i_t(\omega) \tag{6}$$

where $\Delta\omega = (\omega - \omega_o)/(\omega_o), Q_t = (\omega_o L_t)/(R_S + r_{lt})$, and $Q_r = (\omega_o L_r)/(R_L + r_{lr})$. The quality factors Q_t and Q_r denote how strong the mutual coupling near the resonant frequency is. When the quality factor is large, the coupling between two coils is strong at the same distance.

The received power is equal to the consumed power at the load resistor of the Rx coil; hence, it can be expressed as

$$P_L(\omega) = |i_r(\omega)|^2 R_L. \tag{7}$$

Then, we can derive the following equation from (6) and (7):

$$P_L(\omega) = \frac{P_S Q_t Q_r \eta_t \eta_r k^2}{\left(\sqrt{(1 + (2\Delta\omega)^2 Q_t^2)\,(1 + (2\Delta\omega)^2 Q_r^2)} + Q_t Q_r k^2\right)^2} \tag{8}$$

where $P_S = V_t^2/(R_S), \eta_t = R_S/(R_S + r_{lt})$, and $\eta_r = R_L/(R_L + r_{lr})$. Here, P_S is the available transmission power when $\omega = \omega_o$, because the reactance terms are zero at $\omega = \omega_o$. In addition, η_t and η_r are the efficiency of the Tx circuit and the Rx circuit, respectively.

When $w = \omega_o$, (8) is reduced to

$$P_L(\omega_o) = \frac{P_S Q_t Q_r \eta_t \eta_r k^2}{(1 + Q_t Q_r k^2)^2}. \tag{9}$$

From (9), we can calculate the equivalent S_{21} parameter [13], [14]

$$S_{21}(\omega_o) = 2\frac{V_{R_L}}{V_t}\sqrt{\frac{R_S}{R_L}} = 2\sqrt{\frac{Q_t Q_r \eta_t \eta_r k^2}{(1 + Q_t Q_r k^2)^2}}. \tag{10}$$

When the value of the coupling coefficient k is sufficiently small, S_{21} can be approximated as $S_{21} \simeq 2\sqrt{Q_t Q_r \eta_t \eta_r k^2}$. Thus, S_{21} is proportional to $Q_t Q_r$ as well as k [15]. However, the coils become off resonance as k increases beyond a certain value, which is referred to as frequency splitting [16], [17]. We call the coupling coefficient just before frequency splitting occurs as a splitting coupling point and denote it by k_{split}. S_{21} at the resonant frequency decreases with increasing k when $k > k_{\text{split}}$. In contrast, when $k < k_{\text{split}}$, S_{21} at the resonant frequency decreases with decreasing k because of weak coupling. This means that both S_{21} and P_L are maximized at k_{split}.

To find k_{split}, we take the derivative of (10) with respect to k, and find the value of k that satisfies the following conditions: $(\partial S_{21}(\omega_o))/(\partial k) = 0$ and $(\partial^2 S_{21}(\omega_o))/(\partial k^2) < 0$. Then, k_{split} can be obtained as follows [17]:

$$k_{\text{split}} = \frac{1}{\sqrt{Q_t Q_r}}. \tag{11}$$

k_{split} is inversely proportional to the quality factor. This means that strong resonance causes frequency splitting well. In addition, we can determine the maximum S_{21} from (10) and (11):

$$|S_{21}|_{\max} = \sqrt{\eta_t \eta_r}. \tag{12}$$

Here, $|S_{21}|_{\max}$ is equal to 1 if there are no losses in circuits, which would be the case when η_t and η_r are equal to 1.

When $k > k_{\text{split}}$, a resonant frequency is separated into two frequency modes, one higher and the other lower than the original resonant frequency. In this case, the peak points of S_{21} appear at two splitting frequencies instead of at the resonant frequency. Then, the received power near the resonant frequency decreases, which results in serious degradation of the capacity of MI communication that uses the resonant frequency as a central frequency.

To solve this problem, we propose an adaptive frequency-tracking scheme. From coupled-mode theory, the splitting frequencies where the peak points of S_{21} appear can be found as follows [18]:

$$\omega_{\pm} = \omega_o - j\Gamma \pm \frac{\omega_o k}{2} \tag{13}$$

where Γ is the intrinsic decay rate due to absorption and radiated losses. Comparing $S_{21}(\omega_+)$ and $S_{21}(\omega_-)$, the Tx coil can select the frequency $\omega_{\max}$, where the maximum value of S_{21} appears, such that $\omega_{\max} = \max_{\omega_\pm}(S_{21}(\omega_+), S_{21}(\omega_-))$. As the MI communication system uses $\omega_{\max}$ as a central frequency for transmission instead of the original resonant frequency, large capacity can be obtained even in strongly coupled regions.

III. Loosely Coupled Region

A. Two-Coil System

In a loosely coupled region where $k \ll k_{\text{split}}$, frequency splitting is not observed. In such cases, we may neglect the effect of coupling that is seen in the Tx coil.[1] Then, we can obtain $i_t(\omega)$ and $i_r(\omega)$ near the angular resonant frequency as follows:

$$i_t(\omega) = \frac{V_t}{(R_S + r_{lt})(1 + j2\Delta\omega Q_t)},$$
$$i_r(\omega) = \frac{j\omega k\sqrt{L_t L_r}}{(R_L + r_{lr})(1 + j2\Delta\omega Q_r)} \cdot i_t(\omega). \tag{14}$$

[1]This assumption can be verified by comparing Opt-Q (Ana.) with Opt-Q (Sim.) in Figs. 6 and 7 of Section IV.

In the context of the MI communication system, $i_r(\omega)$ can be expressed as $i_r(\omega) = |h|^2 i_t(\omega)$, where $|h|^2$ is the channel gain that $i_t(\omega)$ experiences. Thus, $|h|^2$ can be defined as follows:

$$|h|^2 = \frac{R_S + r_{lt}}{R_L + r_{lr}} \cdot \frac{k^2 Q_t Q_r}{(1 + (2\Delta\omega)^2 Q_t Q_r)}. \tag{15}$$

Here, k can be approximated as a function of the distance between the coils d [9]:

$$k(d) = \frac{a_t^2 a_r^2}{\sqrt{a_t a_r}\left(\sqrt{d^2 + a_t^2}\right)^3}. \tag{16}$$

Then, the channel gain $|h|^2$ can be expressed as

$$|h|^2 = \frac{R_S + r_{lt}}{R_L + r_{lr}} \cdot \frac{a_t^3 a_r^3 Q_t Q_r}{\left(d^2 + a_t^2\right)^3 (1 + (2\Delta\omega)^2 Q_t Q_r)}. \tag{17}$$

In (17), $|h|^2$ is proportional to $1/d^6$. This means that the path loss exponent is 6. This result is consistent with the result in [4]. Channel gain is large at short distances because of strong coupling. In addition, channel gain is large near the resonant frequency due to the term $\Delta\omega$. We may conclude that $\Delta\omega$ reflects the frequency-selective fading effects in MI communication.

Then, the received power $P_L(\omega)$ can be derived as follows:

$$\begin{aligned} P_L(\omega) &= |i_t(\omega)|^2 |h|^2 R_L \\ &= \frac{P_S Q_t Q_r \eta_t \eta_r k^2}{(1 + (2\Delta\omega)^2 Q_t Q_r)^2}. \end{aligned} \tag{18}$$

When $\omega = \omega_o$, the received power is expressed as

$$P_L(\omega_o) = P_S Q_t Q_r \eta_t \eta_r k^2 \tag{19}$$

which is proportional to $Q_t Q_r$ as well as k^2. Large quality factors cause strong coupling near the resonant frequency, and large k also means that the Tx and Rx coils are coupled strongly at short distances.

The largest received power can be obtained when the quality factors of the Tx and Rx coils are the same [10]:

$$Q = Q_t = Q_r. \tag{20}$$

If we consider identical Tx and Rx coils, both (5) and (20) are satisfied simply. In addition, we use the 3 dB bandwidth as the bandwidth B in our system. Here, the 3 dB bandwidth is defined as the range of frequencies in which the spectral power density of signal is greater than the half of its maximum value. Then, from the relation, $P_L(\omega_o - (B)/(2)) : P_L(\omega_o) = (1)/(2) : 1, B$ can be derived as follows [9]:

$$B = \sqrt{\sqrt{2} - 1} \cdot \frac{1}{Q} \cdot f_c \simeq \frac{0.644}{Q} \cdot f_c. \tag{21}$$

As Q increases, the signal resonates with greater amplitude at the resonant frequency but the bandwidth becomes narrow. Thus, B is inversely proportional to Q.

From the Shannon capacity, the capacity of MI communication is expressed as follows:

$$C = B \log_2 \left(1 + \frac{P_L}{B N_0}\right) \tag{22}$$

where N_0 is noise spectral density. In (22), P_L and B are dominant factors for determining capacity. In addition, both P_L and B are functions of Q, so the capacity C is also a function of Q. Using the relation between C and Q, we can find the optimal value of Q that satisfies the following conditions: $(\partial C)/(\partial Q) = 0$ and $(\partial^2 C)(\partial Q^2) < 0$. Then, $Q_{\max}$ is given by

$$Q_{\max} \simeq \frac{3.16}{\sqrt[3]{\alpha}} \quad \text{where} \quad \alpha \simeq \frac{\mathrm{P_S}\eta_t\eta_r \mathrm{k}^2}{0.644 \mathrm{f_c} \mathrm{N_0}}. \tag{23}$$

In (23), $Q_{\max}$ is inversely proportional to k, so $Q_{\max}$ is large at long distances. It is difficult to guarantee received power that is sufficient to support communication at long distances because the signal strength is attenuated severely as d increases. Therefore, in order to make communication possible even at long distances, strong coupling near the resonant frequency is needed. As a result, large Q is better than large bandwidth for maximizing capacity at long distances. When $Q_{\max}$ is determined, the optimal bandwidth and the maximum capacity are also obtained from (21) and (22), respectively. Quality factor can be adjusted to $Q_{\max}$ when Tx and Rx coils are designed before deployment, of which procedures are described as follows. Based on the distance between Tx and Rx coils, k can be estimated as (16), and $Q_{\max}$ can be calculated according to (23). For adjusting $Q_{\max}$, coils should be designed to have the following inductance: $L = (Q_{\max} R)/(\omega_o)$. Depending on the value of the inductance, the capacitance also should be set as $C = (1)/(\omega_o^2 L)$ for tuning the resonant frequency as ω_o. Then, the value of Q can be tuned to $Q_{\max}$ without the change of the resonant frequency. As a result, the maximum capacity can be achieved at a given distance. We called this scheme as an optimal-Q scheme.

B. MI Relay System

In a two-coil system, the received power at the Rx coil decreases in proportion to $1/d^6$, so it is difficult to guarantee large capacity at long distances. This problem can be solved by deploying relay coils between the Tx and Rx coils. The sinusoidal current in the Tx coil induces another sinusoidal current in the adjacent first relay coil through mutual coupling. The induced sinusoidal current in the first relay coil also induces another sinusoidal current in the second relay coil, and so on. In this way, the signal transmitted by the Tx coil is relayed by intermediate relay coils and finally transferred to the Rx coil. The MI relay system and its equivalent circuit model are shown in Fig. 2(a) and (b), respectively. For the sake of simplicity, we consider identical Tx, relay, and Rx coils, each of which has radius a. The coils have the same inductance and capacitance so that they will resonate at the same resonant frequency. The n relay coils are deployed at equal intervals d between the Tx and Rx coils. The total transmission distance between the Tx and Rx coils may be expressed as $D = (n-1)d$. Then, we can also build the node equations from KVL, shown in (24) shown at the bottom

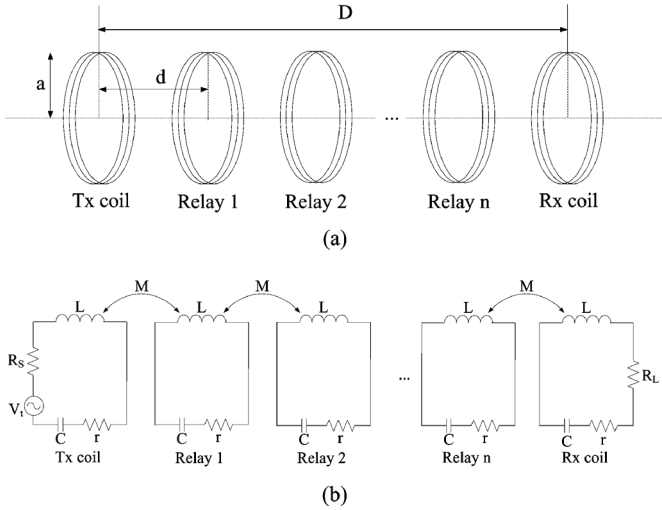

Fig. 2. System model of MI relay system. (a) MI relay system, (b) Equivalent circuit model.

of the page. However, relay coils are used to provide reliable service quality at long distances while they are rarely used at short distances. Thus, we can assume that adjacent coils are coupled loosely. As a result, in the analysis that follows, we can ignore the effect of coupling that is seen in the Tx coil as well as the cross-coupling.[2] Then, the currents in the Tx, relay, and Rx coils are obtained as follows.

$$\begin{aligned}
i_t(\omega) &= \frac{V_t}{(R_S+r)(1+j2\Delta\omega Q)},\\
i_1(\omega) &= \frac{j\omega kL}{r(1+j2\Delta\omega Q)}\cdot i_t(\omega),\\
i_2(\omega) &= \left\{\frac{j\omega kL}{r(1+j2\Delta\omega Q)}\right\}^2\cdot i_t(\omega),\\
&\vdots\\
i_n(\omega) &= \left\{\frac{j\omega kL}{r(1+j2\Delta\omega Q)}\right\}^n\cdot i_t(\omega),\\
i_r(\omega) &= \frac{j\omega kL}{(R_L+r)(1+j2\Delta\omega Q)}\cdot\left\{\frac{j\omega kL}{r(1+j2\Delta\omega Q)}\right\}^n\cdot i_t(\omega).
\end{aligned} \tag{25}$$

[2]This assumption can be verified by comparing Opt-R (Ana.) with Opt-R (Sim.) in Figs. 6 and 7 of Section IV.

Here, k is the coupling coefficient between adjacent coils. Then, the received power is

$$P_L(\omega) = \frac{P_S\eta^2Q^2k^2}{(1+(2\Delta\omega)^2Q^2)^2}\cdot\left\{\frac{Q_{\rm re}^2k^2}{(1+(2\Delta\omega)^2Q_{\rm re}^2)^2}\right\}^n \tag{26}$$

where $Q_{\rm re}$ is the quality factor of relay coils, which can be the same as the quality factor of the Tx and Rx coils by adjusting the inductance and capacitance of the relay coils. If $Q_{\rm re}$ is the same as Q, (26) is reduced to

$$P_L(\omega) = \frac{P_S\eta^2(Q^2k^2)^{n+1}}{(1+(2\Delta\omega)^2Q^2)^{n+2}}. \tag{27}$$

In addition, when $\omega=\omega_o$, the received power is expressed as

$$P_L(\omega_o) = P_S\eta^2(Q^2k^2)^{n+1}. \tag{28}$$

From the relation, $P_L(\omega_o-(B)/(2)) : P_L(\omega_o) = (1)/(2) : 1$, the optimal bandwidth can be obtained as follows:

$$B = \frac{c}{Q}\cdot f_c \quad \text{where } c=\sqrt{\sqrt[n+2]{2}-1}. \tag{29}$$

In addition, from the conditions $\partial C/\partial Q = 0$ and $\partial^2 C/\partial Q^2 < 0$, $Q_{\max}$ may be obtained as follows:

$$\begin{aligned}
Q_{\max} &\simeq \frac{\sqrt[2n+3]{2\cdot\left(e^{w\{-\frac{2n+3}{e^{2n+3}}\}+(2n+3)}-1\right)}}{\sqrt[2n+3]{\alpha}}\\
\text{where } \alpha &\simeq \tfrac{P_S\eta^2k^{2(n+1)}}{cf_cN_0},\ w(x)=\textstyle\sum_{m=1}^{\infty}\frac{(-m)^{m-1}}{m!}x^m.
\end{aligned} \tag{30}$$

Here, $w(x)$ is a Lambert W-function. If there are no relay coils, B and $Q_{\max}$ are the same in a two-coil system. In (30), $Q_{\max}$ increases as k decreases for fixed n. In addition, $Q_{\max}$ increases with increasing n for fixed k. Hence, large Q is also good for maximizing capacity at long distances in MI relay systems.

IV. Performance Evaluations and Discussion

To verify our analysis, we performed simulations using the Agilent ADS. In our simulations, we considered identical Tx, relay, and Rx coils. The radius of coils was 0.1 m, and their internal resistance was 0.55 Ω. In a strongly coupled region, the

$$\begin{aligned}
V_t &= \left(R_S+r+j\omega L+\frac{1}{j\omega C}\right)i_t+j\omega Mi_1+\cdots+j\omega Mi_n+j\omega Mi_r,\\
0 &= j\omega Mi_t+\left(r+j\omega L+\frac{1}{j\omega C}\right)i_1+\cdots+j\omega Mi_n+j\omega Mi_r,\\
&\vdots\\
0 &= j\omega Mi_t+j\omega Mi_1+\cdots+\left(r+j\omega L+\frac{1}{j\omega C}\right)i_n+j\omega Mi_r,\\
0 &= j\omega Mi_t+j\omega Mi_1+\cdots+j\omega Mi_n+\left(R_L+r+j\omega L+\frac{1}{j\omega C}\right)i_r.
\end{aligned} \tag{24}$$

TABLE I
PARAMETERS FOR EVALUATION

Parameters	Values
a_t, a_r	0.1 m
L_t, L_r	4.93 uH
C_t, C_r	51.33 pF
R_S, R_L	10 Ω
r_{lt}, r_{lr}	0.55 Ω
P_S	1 W
f_c	10 MHz
N_0	-103 dBm

inductance and capacitance of coils were 4.93 uH and 51.33 pF, respectively, so that the coils will resonate at the same resonant frequency, 10 MHz. In a loosely coupled region, the inductance of coils is chosen depending on the value of $Q_{\max}$, such as $L = Q_{\max}R/\omega_o$. In addition, the capacitance of coils is chosen depending on the value of inductance, such as $C = 1/\omega_o^2 L$, in order to make the coils resonate at the same frequency of 10 MHz. The source and load resistors were set as 10 Ω and the source power was set as 1 W. In addition, we used the average noise power of soil, which is a dense medium, as the noise spectral density, such that $N_0 = -103$ dBm [4]. Details of the parameters for the performance evaluations are shown in Table I.

Fig. 3 shows the effect of frequency splitting in the strongly coupled region. Here, (Ana.) and (Sim.) are analytical results and simulation results, respectively. In this simulation, the value of k_{split} is 0.034. When k is smaller than k_{split}, the maximum value of $|S_{21}|$ occurs at the resonant frequency. For example, the maximum value of $|S_{21}|$ is 0.94 at 10 MHz when $k = 0.03$. In contrast, when k is larger than k_{split}, resonant modes occur at frequencies higher and lower than the resonant frequency. Therefore, the values of $|S_{21}|$ that occur at 9.6 and 10.5 MHz are larger than the value of $|S_{21}|$ at 10 MHz. The value of $|S_{21}|$ at 10 MHz is 0.57 when $k = 0.1$. This value is smaller than the value of $|S_{21}|$ at 10 MHz when $k = 0.03$. In general, the value of $|S_{21}|$ increases with increasing k, but the value of $|S_{21}|$ decreases as k increases beyond k_{split}. By using an adaptive frequency-tracking scheme, an MI communication system can trace the frequency where the maximum value of $|S_{21}|$ occurs and use it as the central frequency when $k = 0.1$. Then, the value of $|S_{21}|$ achieved in the MI communication system is 0.945 instead of 0.57.

Fig. 4 shows the capacity versus distance between two coils in the strongly coupled region. Here, a conventional scheme uses the resonant frequency as a central frequency at all distances. In addition, the distance, which is corresponding to k_{split}, is 0.3 m; thus, frequency splitting occurs at distances shorter than 0.3 m. As a result, when d is smaller than 0.3 m, the capacity decreases with decreasing d in the conventional scheme. However, in an adaptive frequency-tracking scheme, the Tx coil traces $\omega_{\max}$ of the splitting frequencies on the basis of the measured k and uses $\omega_{\max}$ as the central frequency for the transmission. As a result, the proposed adaptive frequency-tracking scheme can compensate for the degradation of capacity and achieve large capacity even at distances shorter than 0.3 m. When d is greater than 0.3 m, the capacity of both schemes decreases because the received power decreases seriously in proportion to $1/d^6$ with increasing d [4]. In a strongly coupled region, the analytical results are in good agreement with the simulation results.

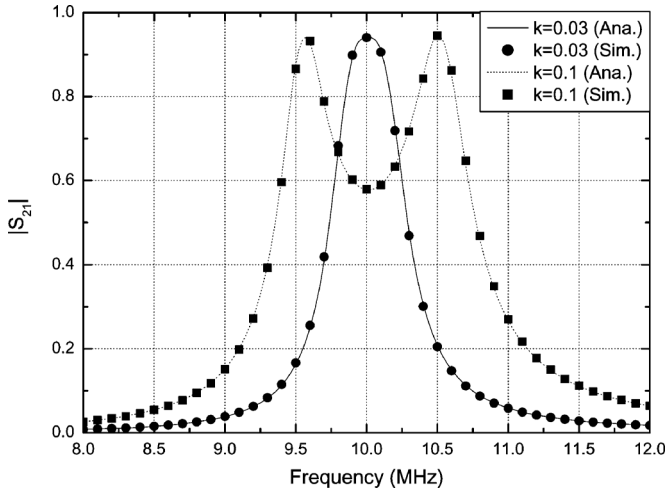

Fig. 3. Effect of frequency splitting in the strongly coupled region.

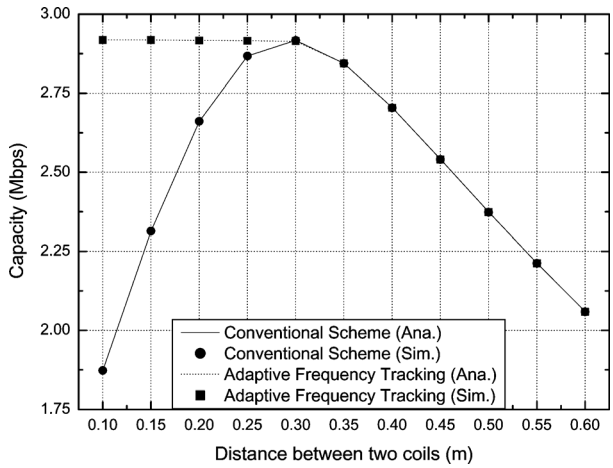

Fig. 4. Capacity versus distance between two coils in the strongly coupled region.

Fig. 5 shows the optimal bandwidth and quality factor versus the distance between two coils in the loosely coupled region. Here, the distance between relay coils is 0.5 m. Opt-Q and Opt-R are the proposed optimal-Q schemes, which adjust the quality factor to the optimal value at a given distance in the two-coil system and the relay system, respectively. The received power is proportional to both Q^2 and k^2, as shown in (19) and (28). Therefore, at short distances, the received power in the Rx coil can be sufficient for communication due to large k, even though Q is small. In addition, smaller Q means larger B. Thus, capacity can be maximized even though the received power is not great, due to small Q but large B. This finding means that large B is more important than the received power for increasing the capacity at short distances. On the other hand, as the distance between two coils increases, the coils are weakly coupled. Then, the received power can be attenuated to a level that is much less than the level required for enabling communication. Thus, large Q, which strengthens resonance near the resonant frequency, is

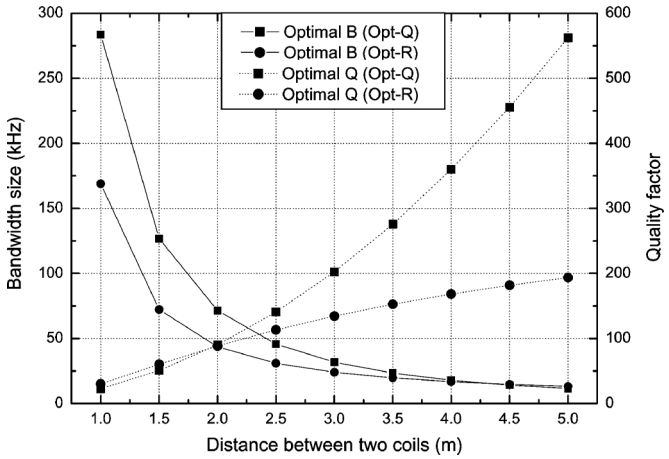

Fig. 5. Optimal bandwidth and quality factor versus distance between two coils in the loosely coupled region.

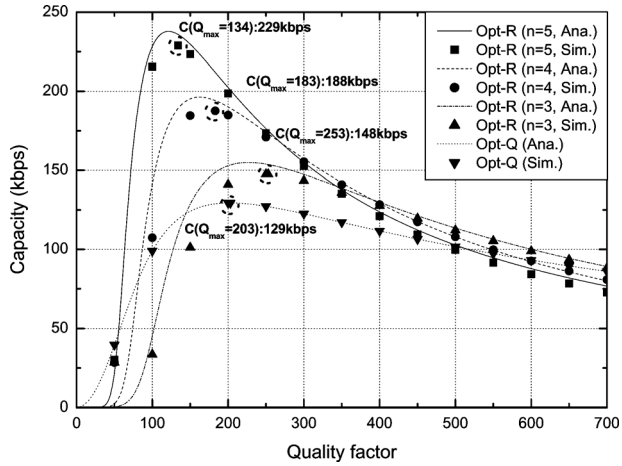

Fig. 6. Capacity versus quality factor when $D = 3$ m in the loosely coupled region.

needed to compensate for the attenuation of the received power so that communication could be possible. As a result, Q increases rapidly, while B decreases with increasing distance. At the same distances, a relay system can achieve greater received power than a two-coil system because the relay coils that are deployed between the Tx and Rx coils support strong resonance. This increase in received power indicates that the relay system can support the power that is needed for communication with smaller Q, compared with the two-coil system. Thus, the relay system uses smaller Q than the two-coil system for maximizing capacity. Further, Q increases gradually with increasing distance in case of the relay system, compared with the two-coil system.

Fig. 6 shows the capacity versus quality factor in the loosely coupled region when the total transmission distance is 3 m. The received power increases greatly as Q increases, so the capacity also increases with increasing Q. However, when Q increases beyond a certain value of Q, B is extremely small even though the received power increases. As a result, the capacity drops gradually with increasing Q. This finding means that the optimal Q, at which capacity is maximized, exists at each distance. In Fig. 6, the black dotted circles are the values of $Q_{\max}$, which are found from (23) and (30). In the two-coil system, the maximum capacity, 129 kb/s, is achieved at the exact value of $Q_{\max}$ obtained from analysis, such that $Q_{\max} = 203$. This is marked as $C_{\text{peak}}(Q = 203) : 129$ kb/s in Fig. 6. In the relay system, signal strength decreases sharply in proportion to $(k^2)^{n+1}$ as the signal goes through the relay coils. When relay coils use large Q for strong magnetic resonance, they can prevent serious attenuation of the signal strength. Therefore, the capacity of a relay system is larger than that of a two-coil system at large Q. However, the capacity of a relay system is similar to that of a two-coil system at extremely large Q because bandwidth becomes very narrow. In contrast, when relay coils use small Q, the magnetic resonance between adjacent coils is not strong enough to compensate for the attenuation of the signal strength. As a result, the capacity of a relay system is smaller than that of a two-coil system at small Q. At the same D, as the number of

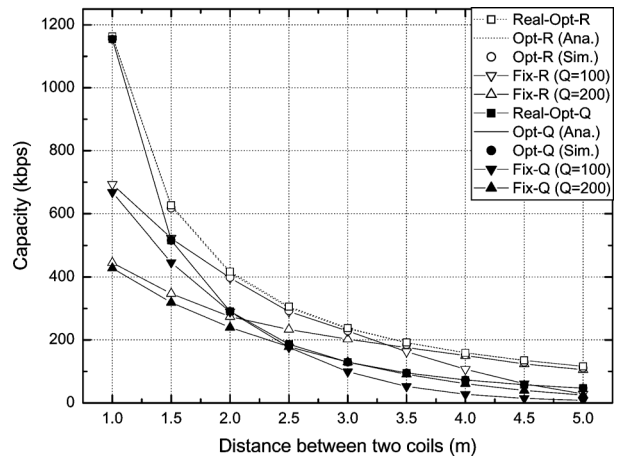

Fig. 7. Capacity versus distance between two coils in the loosely coupled region.

relay coils increases, adjacent coils are coupled strongly. Therefore, the signal transmitted by the Tx coil can be transferred to the Rx coil reliably even with small Q. This indicates that small Q with large B is good for maximizing capacity as the number of relay coils increases, in consequence, the optimal Q of Opt-R becomes small at large n. In the relay system, there are some differences between the analytical results and the simulation results as the number of relay coils increases because of strong coupling between adjacent coils, but the analytical results are relatively well matched to the simulation results. Therefore, our assumptions are valid for the loosely coupled region. In addition, the optimal Q, at which the maximum capacity is achieved, is in agreement with $Q_{\max}$ obtained numerically.

Fig. 7 shows the capacity versus distance between two coils in the loosely coupled region. Here, Real-Opt-Q and Real-Opt-R are the optimal capacity for both two-coil and relay systems, respectively. The optimal capacity could be found from the exhaustive search over all values of quality factor. In addition, we compare the performances of the optimal-Q schemes with those of conventional fix-Q schemes that use a predetermined value

of Q at all distances. The optimal-Q schemes achieve near-optimal capacity at each distance by tuning the optimal Q. However, fix-Q schemes achieve near-optimal capacity at only a particular distance, at which the optimal value of Q is similar to the value of Q that fix-Q schemes use. For example, a fix-Q scheme in which Q is 100 achieves near-optimal capacity when $d = 2$ m, at which distance the optimal value of Q is 90. As the distance changes, the performance of the fix-Q scheme decreases because the difference between its own Q and the optimal Q is large. As the total transmission distance between the Tx and Rx coils increases, a relay system improves capacity significantly over a two-coil system according as the number of relay coils increases. In addition, the analytical results are well matched to the simulation results.

V. Conclusion

The use of magnetic induction is an excellent way of achieving wireless communication in embedded sensor networks. Herein, we studied how to maximize system capacity when using MI communication. In a strongly coupled region, we considered frequency splitting, which causes the Tx and Rx coils to be out of resonance, thereby reducing the strength of the received signal seriously in the Rx coil. To compensate for the serious degradation of capacity in such a situation, we found the value of the coupling coefficient just before frequency splitting occurs and proposed an adaptive frequency-tracking scheme. In a loosely coupled region, we provided a channel model that includes path loss and fading. Using the derived channel model, we analyzed the optimal quality factor for maximizing the capacity at a given distance in both a two-coil system and a relay system. The optimal quality factor depends on the distance between coils, so we proposed an optimal-Q scheme to achieve the maximum capacity at a given distance. In addition, through performance evaluations using the Agilent ADS simulations, we showed the accuracy of the analytic results and the effectiveness of our schemes.

Acknowledgment

This research was supported by the KCC (Korea Communications Commission), Korea, under the R&D program supervised by the KCA (Korea Communications Agency) (KCA-2013-11-911-04-001).

References

[1] T. Yamazaki, "The ubiquitous home," *Int. J. Smart Home*, vol. 1, no. 1, pp. 17–22, Jan. 2007.
[2] I. F. Akyildiz and E. P. Stuntebeck, "Wireless underground sensor networks: Research challenges," *Ad Hoc Netw. J.*, vol. 4, no. 6, pp. 669–686, Apr. 2006.
[3] L. Li, M. C. Vuran, and I. F. Akyildiz, "Characteristics of underground channel for wireless underground sensor networks," in *Proc. IFIP Mediterranean Ad Hoc Netw. Workshop (Med-Hoc-Net)*, Jun. 2007, pp. 92–99.
[4] Z. Sun and I. F. Akyildiz, "Magnetic induction communications for wireless underground sensor networks," *IEEE Trans. Antenna Propag.*, vol. 58, no. 7, pp. 2426–2435, Jul. 2010.
[5] R. Bansal, "Near-field magnetic communication," *IEEE Antennas Propag. Mag.*, vol. 46, no. 2, pp. 114–115, Apr. 2004.
[6] V. A. Kalinin, K. H. Ringhofer, and L. Solymar, "Magneto-inductive waves in one, two, and three dimensions," *J. Appl. Phys.*, vol. 92, no. 10, pp. 6252–6261, Nov. 2002.
[7] R. R. A. Syms, I. R. Young, and L. Solymar, "Low-loss magneto-inductive waveguides," *J. Phys. D, Appl. Phys.*, vol. 39, no. 18, pp. 3945–3951, Sept. 2006.
[8] Z. Sun and I. F. Akyildiz, "Deployment algorithms for wireless underground sensor networks using magnetic induction," in *Proc. IEEE Global Telecommun. Conf. (IEEE GLOBECOM)*, Dec. 2010, pp. 1–5.
[9] H. Jiang and Y. Wang, "Capacity performance of an inductively coupled near field communication system," in *Proc. Int. Symp. IEEE Antennas Propag. Soc. (AP-S)*, Jul. 2008, pp. 1–4.
[10] J. I. Agbinya and M. Masihpour, "Power equations and capacity performance of magnetic induction body area network nodes," in *Proc. Broadband Biomed. Commun. (IB2Com)*, Dec. 2010, pp. 1–6.
[11] B. Rose, "Home networks: A standard perspective," *IEEE Commun. Mag.*, vol. 39, no. 12, pp. 78–85, Dec. 2001.
[12] A. Kurs, A. Karalis, R. Moffatt, J. D. Joannopoulos, P. Fisher, and M. Soljacic, "Wireless power transfer via strongly coupled magnetic resonances," *Sci. Express*, vol. 317, no. 5834, pp. 83–86, Jul. 2007.
[13] R. Mongia, *RF and Microwave Coupled-Line Circuits*. Norwood, MA, USA: Artech House, 2007.
[14] J. Chen, *Feedback Networks: Theory and Circuit Application*. Singapore: World Scientific, 2007.
[15] C.-J. Chen, T.-H. Chu, C.-L. Lin, and Z.-C. Jou, "A study of loosely coupled coils for wireless power transfer," *IEEE Trans. Circuits Syst. II, Exp. Briefs*, vol. 57, no. 7, pp. 536–540, Jul. 2010.
[16] Y. D. Tak, J. M. Park, and S. W. Nam, "Mode-based analysis of resonant characteristics for near-field coupled small antennas," *IEEE Antennas Wireless Propag. Lett.*, vol. 8, pp. 1238–1241, Nov. 2009.
[17] A. P. Sample, D. T. Meyer, and J. R. Smith, "Analysis, experimental results, and range adaptation of magnetically coupled resonators for wireless power transfer," *IEEE Trans. Ind. Electron.*, vol. 58, no. 2, pp. 544–554, Feb. 2011.
[18] H. A. Haus, *Waves and Fields in Optoelectronics*. Englewood Cliffs, NJ, USA: Prentice-Hall, 1984.